



Contribution of electrical prospecting and spatiotemporal variations to groundwater potential in coastal hydro-sand beds: a case study of Akwa Ibom State, Southern Nigeria

Nyakno Jimmy George¹ · Okechukwu Ebuka Agbasi² · James Anthony Umoh¹ · Aniekan Martin Ekanem¹ · Jude Steven Ejepu³ · Jewel Emem Thomas¹ · Ifioke Efiang Udoinyang⁴

Received: 26 October 2022 / Accepted: 1 December 2022

© The Author(s) under exclusive licence to Institute of Geophysics, Polish Academy of Sciences & Polish Academy of Sciences 2022

Abstract

The current study used vertical electrical sounding (VES), borehole (BH) data, Remote Sensing (RS), and Geographic Information System (GIS) techniques to identify groundwater potential zones in the coastal area of Akwa Ibom state, Nigeria, for the first time. This research aimed at producing groundwater potential zone map that can divide the study region into separate zones based on their groundwater potential ranking. The deployed method integrated VES procedure utilizing the Schlumberger electrode configuration some core samples for estimation of porosity, Satellite Shuttle Radar Topography Mission (SRTM), Digital Elevation Model (DEM), which served as input data for RS and GIS. Thematic maps of lineament density, lithology, land use and land cover, drainage density, and slope were created as GIS layers in a geo-database. Weightages were assigned based on a pair-wise assessment of the components that appear to be essential in retaining, storing, and transporting groundwater. The Analytical Hierarchy Process (AHP) was used in a GIS setting to merge five thematic maps of elements controlling groundwater occurrence and movement using weighted overlay. Results show that aquifers with high thickness and depths are clustering around VES 9, VES 14, and VES 15 that have the highest aquifer thickness in the range of 219–262 m and the highest aquifer depth in the range of 222.09–264.74 m. The highest aquifer resistivity in this area ranges from 2963 to 3683 Ω m. The hydraulic conductivity of the area is highest around the south-eastern part of the study area, with maximum value of 3.43 m/day. The transmissivity increases in the northern part of the study area, while the eastern parts showed the lowest values. The highest aquifer resistivity in this area ranged from 2963 to 3683 Ω m. Inference from analysis indicated that the most important element was soil type (43%), followed by lineament density (33%) and slope (13%). Land use/land cover was discovered as a marginal contributor to groundwater in the research region, accounting for about 4% of the total contributors. The study *CR* determined to be 0.043884, is much lower than the 0.10 consistency threshold and hence the justification of the results. The result of the overlay of the geophysical survey on the groundwater potential zones obtained from the RS, GIS, and VES techniques done in the first time in the study area has shown seamlessly that the study area has high groundwater prospectivity for subsistent and commercial extractions.

Keywords AHP · Aquifer · Groundwater potential · Spatiotemporal variations · Sand beds

Edited by Dr. Michael Nones (CO-EDITOR-IN-CHIEF).

✉ Nyakno Jimmy George
nyaknojimmy@gmail.com; nyaknogeorge@aksu.edu.ng

¹ Department of Physics (Geophysics Research Group), Akwa Ibom State University, Mkpatt Enin, PMB 1162, Uyo, Nigeria

² Department of Physics, Michael Okpara University of Agriculture, Umudike, Nigeria

³ Department of Geology, Federal University of Technology, Minna, Nigeria

⁴ Department of Physics, Rhema University Nigeria, Aba, Nigeria

Introduction

Water is a fundamental natural resource that exists as both surface water and groundwater. The development and growth of any society is contingent on the availability and utilization of appropriate water. Water covers almost two-thirds of the world's total land area (Agbasi and Etuk 2016). This essential resource, which is often sparse, plentiful, yet unevenly distributed in geography and time is critical to human survival. Groundwater is water that has penetrated into the soil directly via precipitation, recharge from streams and

other natural water sources and man-made recharge (Ibuot et al. 2022). More than 1.5 billion people worldwide are reported to rely on groundwater for their drinking water needs. Groundwater occurrence, distribution, and flow are discontinuous and governed by the dynamic interplay of numerous environmental elements such as geology, slope, overburden thickness, and weathering (Agbasi et al. 2019; George et al. 2021).

Despite the fact that the nineteenth and twentieth centuries saw significant industrial and economic revolutions, many developing nations (including Nigeria) are still unable to provide enough potable water for their citizens (Oli et al. 2021). For example, with an expanding population and industrialization, demand for water resources in Nigeria is continually increasing, forcing residents to rely on drinking water from wells. More than 70% of accessible drinkable water in Nigeria is tapped from the ground, with the exception of Abuja, where more than 80% of the municipal area is connected to a pipe-borne water network (George et al. 2015a; b; Abdullateef et al. 2021; Ejepu et al. 2022). As a result, the importance of groundwater in supplying a bigger share of water demand cannot be overstated. Although it is possible to identify groundwater potential through observation wells, it is uneconomical or expensive in extensive areas. Many multivariate statistically based techniques, which do not require field work, have been used by researchers to estimate groundwater potential. Such techniques include decision tree model (Lee and Lee 2015), logistic regression model (Pourtaghi and Pourghasmi 2014) and the principal component analysis (PCA) (Helena et al. 2000). Alternatively, the diagnostic hierarchy process (AHP) is viewed to be a simple, consistent, valuable, obvious and dependable technique (Machiwal et al. 2011). The AHP approach is a straightforward and a matching technique that can be integrated with geographic information system (GIS) and remote sensing (RS) data for local and regional groundwater potential studies. Groundwater parameters such as precipitation, aquifers, land use, and soil type can easily be defined as spatial data in a GIS environment. Groundwater systems are made up of a complex web of interactions between the physical environment (soils, geology, precipitation, vegetation, and terrain) and the social and economic activities that put pressure on the physical environment (Ejiogu et al. 2019). The study is provoked by inadequate understanding about the geographical units responsible for groundwater occurrence, migration, and storage. As a result, geospatial groundwater assessment associated with qualitative and quantitative considerations is required to offer a better knowledge of groundwater dynamics for sustainable usage.

Several land and water management strategies have emerged, and remote sensing and Geographic Information Systems (GIS) have gained popularity. The availability of

free-to-low-cost satellite imagery and digital elevation models is the most significant contribution of remote sensing technology to groundwater exploration (Abdulrazzaq et al. 2020; Ige et al. 2020). GIS is an important tool that can manage vast amounts of data (both geographical and spatial) and can enable a variety of quantitative and qualitative spatial analyses and interpretations (Aladeboyeje et al. 2021). This research project is primarily aimed at producing and characterizing groundwater potential maps that can classify the study area into separate zones based on their groundwater potential. To this end, the novelty in this work involves the use of local information from surface geophysical technique and regional/spatiotemporal information from GIS-based multicriteria decision making (MCDM) and AHP methods to produce groundwater-potential maps of the study area using logical groups of characterizing hydrogeological entities. The resulting detailed map of the area can be utilized as inputs for understanding the hydrogeological systems of the study area and as data for future research (Adiat et al. 2012; Ejepu et al. 2020; Aretouyap et al. 2022). The generated, collected, and digitized data were organized into logical groups of entities with characterizing geological factors (lithology and lineament), drainage density, and physiographic factors (slope, land use/land cover) according to Ekanem et al. (2022a) to produce a properly organized geo-database capable of allowing responsible officers, stakeholders and subsequent researchers to make decisions and reviews for water resource extraction, monitoring and management.

Location and geology of the study area

The digitized map of Fig. 1 shows that the study area covers Ibeno, Mkpat Enin, Onna and Eket Local Government Areas (LGAs) of Akwa Ibom State, which stretch out from longitudes 7.68° to 8.35° E and latitudes 4.25° to 4.90° N in the southern parts of Akwa Ibom state and are active shoreline regions within the Gulf of Guinea. Geologically, the study area is part of the Benin Formation, which consists of Coastal Plain sands. The general geology of the study area is primarily Coastal Plain sand (Benin Formation) deposits, and the landscape is averagely flat. It is a deposition of deltaic, estuarine, lagoonal, fluvial-lacustrine and marine materials by its locations (Short and Stauble 1967; George et al. 2014; Ibuot et al. 2013; George 2021a, b). A few LGAs have fairly undulating landscape occasioned by isostatic compensation provoked by gravitational pull energized by the Niger Delta Basin that is actively collapsing. These areas are as high as 60,000 mm above mean sea level owing to the impact of the Atlantic Ocean and its concomitant rivers and valleys (Ibanga and George 2016). The aquifer is made up of both closed and open hydrogeologic unit, with varied

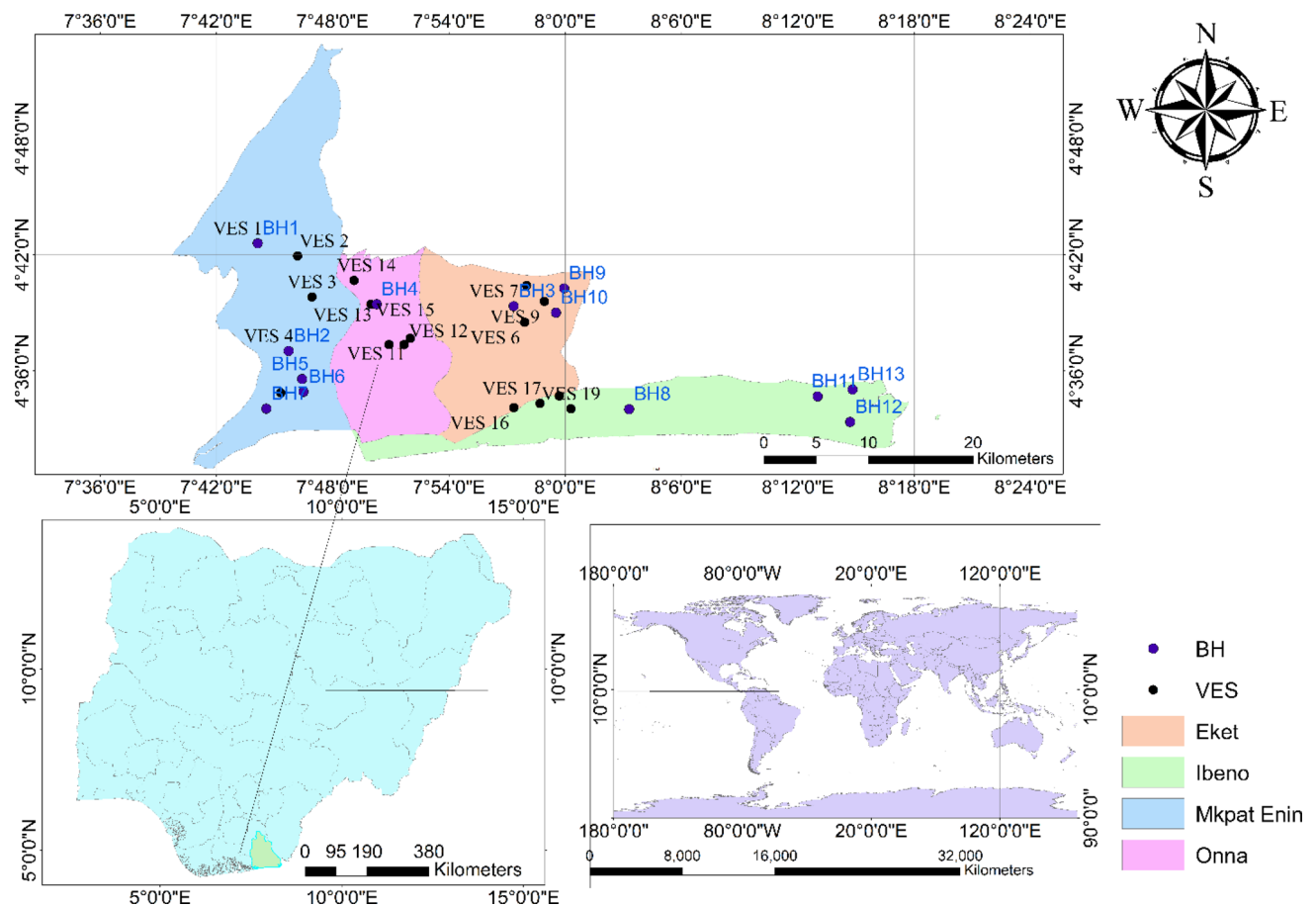


Fig. 1 Map of the world, Nigeria, and the study location showing study locations with BH and VES points

levels of salinity in groundwater. The continental flood plain sands and its alluvial deposits have modest to high rate of permeability and porosity. Salt water incursion into sedimentary aquifers occurs under the fresh water lens, which stretches out by about 5 km to the shore. The main hydrogeologic units in the region are Coastal Plain Sands interspersed with poorly sorted continental (fine-medium-coarse) sands and gravels. The suite of sands alternate with thinly clayey sands, lignite streaks and lenses (George 2021b). The spread of aquifer sands is cut off by the thin argillaceous layers. This gives rise to the formation of multi-aquifer systems throughout the region.

Sediments in the study area have grain sizes ranging from coarse to fine, and they are unevenly and poorly sorted, with a large thickness and a negligible quantity of clay, silt, and sandstone with various sequences that correspond to separate aquifers of varying thicknesses. The upper sandy aquifer has composition of alluvial materials such as gravel, fine- to medium-grained carbonaceous sand or unconsolidated sands of various grades (Reijers et al. 1997; Akpan et al. 2013).

Materials and methods

VES technique

The basic lithological sand-bed characteristics known as primary geo-electric indices in the study area were estimated using data gathered from vertical electrical sounding survey at different locations. The Schlumberger electrode configuration arrangement employed through the deployment of terrameter and its accessories to measure and record the subsurface resistances (George 2020; Aizebeokhaia et al. 2021) was chosen due to its ability sensitivity to the vertical and lateral section of the soil profiles. The study uses a surface geophysical survey from nineteen locations within the Akwa Ibom State coastal zone, which serve as potential prolific hydrogeological units for groundwater abstraction. The Schlumberger electrical resistivity configuration employed deduced the bulk resistivity through the direct measurement of resistance

from the instrument by current injected into the ground (Inim et al. 2020; Thomas et al. 2020; George et al. 2022). The current potential fields (delivered to the ground) were measured using two pairs of electrodes, each corresponding to a potential electrode (MN) and current electrode (AB). For assurance of quality in the field measurements, straight lines were maintained in both the outer (current) and inner (potential) electrode separations. Besides, about one-third of the electrodes were driven into the earth with assured grip between the metal electrodes and the ground (Obinawu et al. 2011; George et al. 2016). MN varied from 0.5 m at AB = 2 m up to 40 m at AB = 600 m (Akpan et al. 2013; Ibuot et al. 2013).

Apparent resistance (R_a) measured from the Schlumberger electrode configuration arrangement was used with geometric factor $G = \pi \left[\frac{(AB/2)^2 - (MN/2)^2}{MN} \right]$ to compute apparent resistivity (ρ_a) values through Eq. (1):

$$\rho_a = \pi \left[\frac{(AB/2)^2 - (MN/2)^2}{MN} \right] R_a. \quad (1)$$

The processing of the measured resistivity data began by smoothing using the log–log plot of ρ_a against (AB/2), followed by electronic processing, which involved the use of WinResist software program (Vander Velpen and Sporry 1993). The data processed manually to remove outliers were electronically processed quantitatively using a 1-D least square computer-aided forward modelling software program known as WINRESIST. With the constraints of nearby ground truth data, the software program furnished the interpreted curves by distinguishing the primary geoelectric indices such as layer resistivity, thickness and depth, in which their respective aquifer values are shown in (Table 1). The goodness of fit established through the matching of field data with theoretical values iteratively was manifested in the achieved root mean square errors (RMSE) generally found to be < 5 (see Fig. 2).

Aquifer, a body of rocks/or sediments that holds water, is drenched rocks or geological units through which volumes of fluid/water transmits into springs and wells. In nature, these trenched rocks possess high degree of variability, which practically describes its hydraulic properties (Obiora et al. 2016). The measurement of aquifer water levels is achieved through indirect measurement, which is used in determining the direction of ground water flow, and in measuring the aquifer hydraulic properties (George 2021a, b). Geo-electrical technology, which is cost-effective, compared to the traditional pumping test is intelligibly pragmatic with promising results (Ekanem et al. 2022a, b; Ikpe et al. 2022; Abdulrazzaq et al. 2022). These parameters are central in determining the flow of water in nature through the aquifer systems and their reaction to fluid extraction. The flow of groundwater through the strata and their release from storage

within the strata govern the response to changes in their supply from the natural stockpile (Ekanem et al. 2020). The measurements of these parameters were achieved with the aid of aquifer samples.

Measurements from cored samples

Porosity

Cored samples collected during borehole drilling at sundry coastal points close to the VES points were employed to deduce porosity and hydraulic conductivity. The samples were sufficiently soaked in distilled water to remove any potential salt contaminant that could influence the pores of the geological samples and possibly the porosity determination. The clean samples were dried with oven so that extraneous fluid within the pores can be removed. Thereafter, the bulk density (B_d) of each of the samples was estimated through the soil weighted mass (Wm)-volume equivalent (VE) ratio of the dry samples as given in Eq. (2):

$$B_d = \frac{Wm}{VE}. \quad (2)$$

With the soil particle density (P_d), ranging from 2.60 to 2.75 g/cm³ with constant mean value of 2.65 g/cm³ (Umoh et al. 2022), the fraction of aquifer pore space, otherwise known as porosity (φ), was estimated and is recorded in Table 2 for each location in the nearby VES station using Eq. (3):

$$\varphi = \left(1 - \frac{B_d}{P_d} \right). \quad (3)$$

Hydraulic conductivity

Using the same cored samples, the hydraulic conductivity, an important property of rock/soil units, was estimated using the constant flow head permeameter (Fig. 3) according to Todd (1980). Constant and continuous supply of water via the inlet provoked steady flow of water through sample with area A (Fig. 3). Stop clock was deployed to record the time (t) of water flow until the volume (V) flowing through the soil sample is 100 cm³ (Fig. 3). Here, different samples are believed to have varying rate of flow based on their pore space/porosity and the consequent permeability (Todd 1980; Obiora et al. 2015). The constant flow head permeameter allowed the determination of the hydraulic conductivities of unconsolidated different soils under the low heads. Figure 3 is made up of aquifer sample of length L and area of cross section A , sandwiched between two leaky plates in a cylindrical tube under a constant-head differential h . The steady water from reservoir

Table 1 Summary of geo-sounding statistics in the study area

VES No	Location	Long. (deg.)	Lat. (deg.)	Elevation (m)	Layer Resistivity (Ohm-m)					Layer thickness (m)			Layer depth (m)		
					ρ_1	ρ_2	ρ_3	ρ_4	h_1	h_2	h_3	d_1	d_2	d_3	
1	Mkpat Enin 1	7.73528	4.70975	30	1408.5	681.5	2619.8	459.8	2.1	7.9	73.3	2.1	10.1	83.4	
2	Mkpat Enin 2	7.769778	4.698972	29	1040.6	491.7	1963.2	-	5.7	80.5	-	5.7	86.2	-	
3	Mkpat Enin 3	7.782222	4.663639	34	1532.6	80.7	987.1	-	36.3	54.7	-	36.3	90.9	-	
4	Mkpat Enin 4	7.762167	4.617083	26	255.1	1440.7	226.2	710	1.0	8.0	56.2	1.0	9.0	65.3	
5	Mkpat Enin 5	7.75525	4.581167	17	757.5	193.6	419.7	1188.0	2.2	12.0	151.2	2.2	14.2	165.4	
6	Eket 1	7.965167	4.641833	19	258.2	1300.7	568.5	-	1.4	49.8	-	1.4	51.2	-	
7	Eket 2	7.955778	4.655694	31	186.8	599.5	1301.7	321.2	1.4	13.5	72.2	1.4	14.9	87.1	
8	Eket 3	7.966778	4.6735	20	318.9	970.5	273.9	-	2.6	247.7	-	2.6	250.0	-	
9	Eket 4	7.982083	4.659806	30	376.1	48.6	1502.6	512.4	0.8	14.5	93.9	0.8	15.2	109.1	
10	Eket 5	7.848472	4.622694	30	192.3	3688.7	1085.9	-	4.4	103.8	-	4.4	108.0	-	
11	Onna 1	7.866722	4.628083	21	1320	3576.5	1235.9	-	11	83.7	-	11	94.7	-	
12	Onna 2	7.861444	4.622639	14	120.8	2560.6	707.2	-	2.5	136.2	-	2.5	136.0	-	
13	Onna 3	7.837889	4.657361	22	416.6	99.3	1810.5	730.8	2.3	8.6	79.5	2.3	10.9	90.5	
14	Onna 4	7.818444	4.677861	25	355.4	85.1	795.7	-	2.1	262.6	-	2.1	265.0	-	
15	Onna 5	7.832889	4.657278	23	174.6	1093.2	2984.5	921.7	3.1	29.2	213.1	3.1	32.3	245.4	
16	Eastern Obolo 1	7.748861	4.560889	17	236.5	114.1	1273.2	-	10.2	63.1	-	10.2	73.3	-	
17	Eastern Obolo 2	7.741111	4.5415	16	21.0	558.8	167.4	-	29.9	208.6	-	29.9	239.0	-	
18	Eastern Obolo 3	7.750047	4.527861	17	279.0	26.3	530.5	-	0.9	65.6	-	0.9	66.5	-	
19	Eastern Obolo 4	7.759833	4.524917	13	484.2	157.8	686	61.6	1.6	10.6	42.8	1.6	12.3	55.0	
Mean				22.8	512.4	935.2	1112.6	543.0	7.2	66.2	93.2	7.2	37.8	105.9	
Range				13.0–34.0	21.0–1532.6	26.3–3688.7	167.4–2984.5	61.6–1188	1.0–36.3	8.0–247.7	52.6–151.2	1.0–36.3	9.0–250	63.9–165.4	

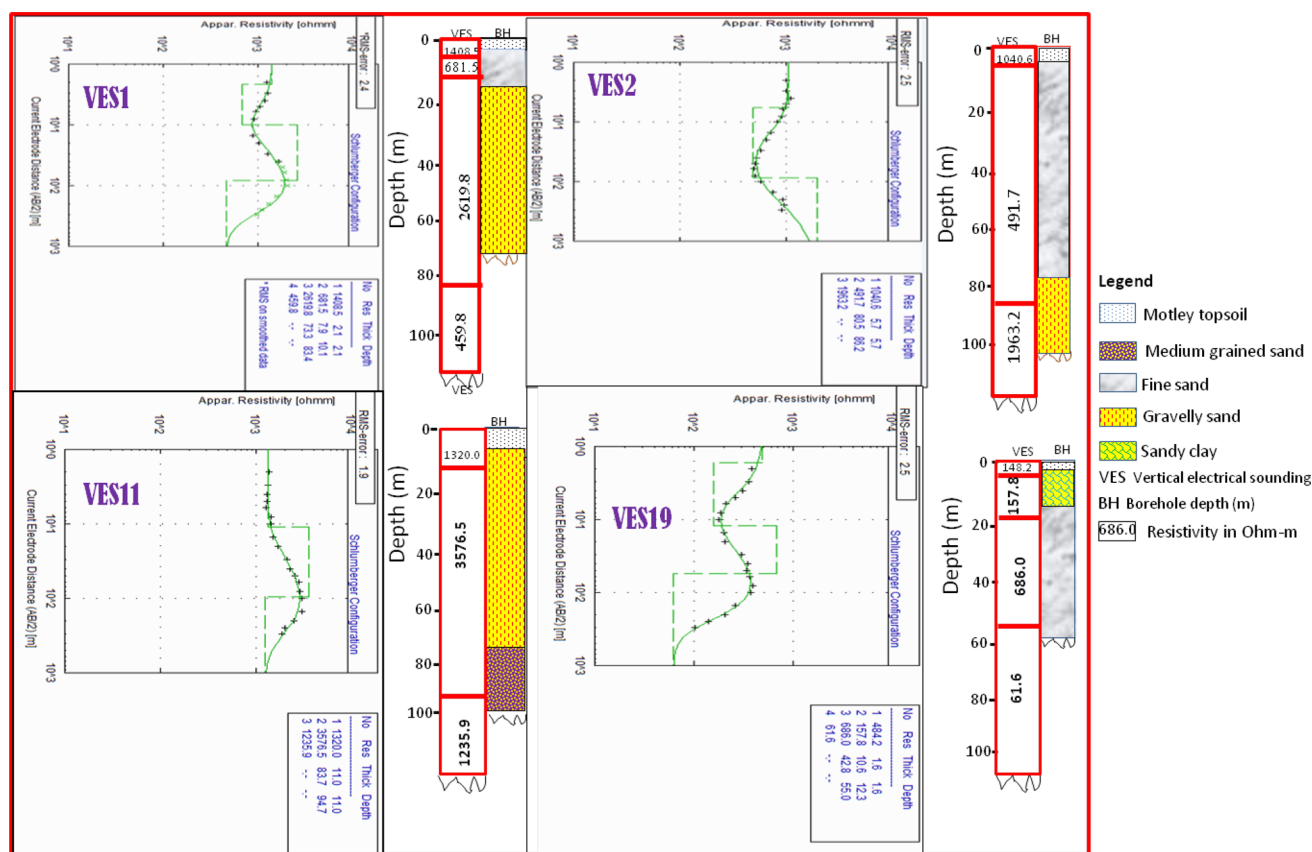


Fig. 2 Sampled correlations of VES 1, 2, 11 and 19 curves with their contiguous lithological log in the study area

Table 2 Measurement scale of AHP (Saaty 1980)

Scale	Definition	Explanation
1	Equal importance	Two elements contribute equally to the objective
3	Moderate importance	Experience and judgment slightly favor one element over another
5	Strong importance	Experience and judgment strongly favor one element over another
7	Very strong importance	One element is favored very strongly over. Its dominance is demonstrated in practice
9	Extreme importance	The evidence favoring one element over another is of the highest possible order of affirmation
2,4,6,8	Intermediate value between the two adjacent judgments	Can be used to express intermediate values

supply entered the medium cylinder from the base and was collected after passing upward through the aquifer sample as overflow (Tang et al. 2017). Based on the setup, hydraulic conductivity K_h , which is a measure of the ease of a medium to transmit fluid (Agbasi and Etuk 2016; George 2020), was estimated for each aquifer sample. The values were computed according to Eq. (4) in m/s and converted to m/day as given in Table 2.

$$K_h = \left(\frac{V \times L}{A \times h \times t} \right). \quad (4)$$

Transmissivity (T)

According to Massoud et al. (2010), K_h and T values play a significant role in aquifer system categorization. These properties generally rate the ease of an aquifer to transmit water over a unit thickness of hydraulic conductivity and across the entire drenched thickness of the aquifer. Often times, they are estimated from pumping tests. Practically, saturated thickness and hydraulic conductivity are used to estimate transmissivity. The mean value of hydraulic conductivity of each layer was multiplied by the inverted thickness of aquifer from 1-D resistivity inversion

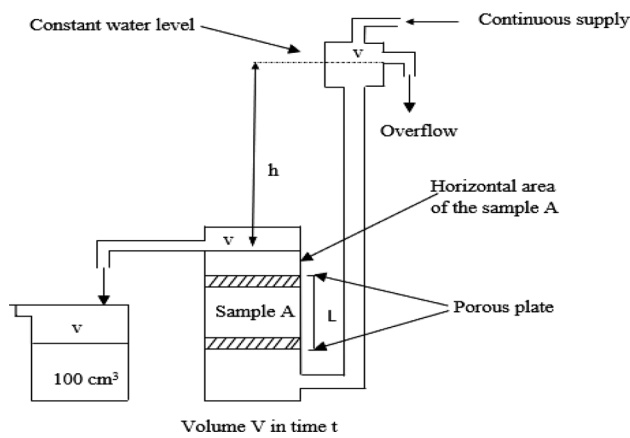


Fig. 3 Permeameter for measuring hydraulic conductivity of aquifer sample by constant flow head method (Todd 1980)

according to Younger (2007) in order to obtain transmissivity recorded in Table 3.

$$T = K_h \times h \tag{5}$$

Remote sensing (RS) and geographic information systems (GIS)

The Satellite Shuttle Radar Topography Mission (SRTM) and Digital Elevation Model (DEM) data were used for the

spatiotemporal investigation. The photographs and datasets were chosen depending on their availability. The satellite gathers photographs of the Earth on a 16-days repetition cycle, using the global reference system-2 as a reference (Aladeboyeje et al. 2021). The scene spreads approximately 170 km north–south by 183 km east–west. Landsat 7's ETM + sensor improved on previous Landsat instruments by adding two new spectral bands: a deep blue visible channel (band 1) specifically designed for water resources and coastal zone investigation; and a new infrared channel (band 9) for detecting cirrus clouds. Two thermal bands (TIRS) collected data with a minimum resolution of 100 m, although they are registered and transmitted with the 30-m data package. ArcGIS 10.8 was used to produce and combines several thematic layers required for identifying relevant groundwater potential locations as well as conducting groundwater studies.

Preprocessing of GIS/RS

The remote sensing data were geometrically adjusted prior to analysis. The bands and pictures from Landsat 8 were layered and mosaicked. The mosaicked picture was clipped using the extract tool in ArcGIS through the Akwa Ibom state shapefile. As with Landsat 8, the SRTM DEM was produced as a mosaic and subset of the research region.

Table 3 Summary probable and economic aquifer system at various VES stations surveyed

VES	Thickness (h) (m)	Depth d (m)	Bulk Resistivity ρ (Ω m)	Porosity ϕ	Hydraulic Conductivity K_h (m/day)	Transmissivity T (m ² /day)
1	73.3	83.4	2619.8	0.4064	2.976	218.1408
2	80.5	86.2	491.7	0.4392	2.637	212.2785
3	54.7	90.9	80.7	0.3928	1.867	102.1249
4	56.2	65.3	266.2	0.3687	3.085	173.377
5	151.2	165.4	419.7	0.423	1.944	293.9328
6	49.8	51.2	1300.7	0.4234	1.431	71.2638
7	72.2	87.1	1301.7	0.3992	1.422	102.6684
8	247.7	250	970.5	0.4283	2.776	687.6152
9	93.9	109.1	1502.6	0.3981	2.42	227.238
10	103.8	108	3688.7	0.3913	1.805	187.359
11	83.7	94.7	3576.5	0.4298	1.113	93.1581
12	136.2	136	2560.6	0.397	2.771	377.4102
13	79.5	90.5	1810.5	0.4298	2.818	224.031
14	262.6	265	85.1	0.3953	1.509	396.2634
15	213.1	245.4	2984.5	0.3875	0.857	182.6267
16	79.2	80.1	211.5	0.4487	2.69	213.048
17	170	182	226.6	0.4279	1.916	325.72
18	95	97.9	235	0.4242	3.415	324.425
19	118.7	122	100.1	0.4558	3.439	408.2093

Preparation of the thematic layers

The number of thematic layers employed is determined by the availability of data in the research region. Five thematic layers, including slope, land use/cover, soil type, drainage and lineament density, were identified as efficient parameters to estimate groundwater potential zones.

Slope map

A slope is a geomorphologic characteristic that influences the infiltration and recharging of a groundwater system in a specific location, and it is measured in degrees. In terms of groundwater, flat locations with low slope store rainfall, which enables recharging, whereas elevated places with high slope have considerable run-off and poor infiltration (Makonyo and Msabi 2021), leading to low groundwater. The slope map for the research region was created using the spatial analyst tool in the ArcGIS 10.8 environment, and it was afterwards classified prior to the overlaying procedure for groundwater mapping.

Land use/cover

Another factor influencing groundwater occurrence is land use and cover. Land cover/use has an influence by either lowering runoff or facilitating or by retaining water on their leaves. Water droplets caught in this manner fall to the earth and refresh the groundwater. Land use/cover may also have a detrimental impact on groundwater through evapotranspiration, assuming steady interception (Biswajit et al. 2020). The land use and coverage of the study have a combination of built-up, vegetation, barren land, agricultural area, and water bodies. Visual interpretation was used to create an overview of the land use and land cover. For the final land-use map, supervised classification (maximum likelihood classifier) was used using the proper band combinations. The resultant map was then classed in order to delineate groundwater potential.

Soil type

The lithology, stratigraphy, and structure of the geological strata present affect the presence of groundwater as well as the extent and distribution of aquifers and aquitards in an area. The porosity and permeability of aquifer rocks are both influenced by soil type. The soil type map for the research region was digitized from an Akwa Ibom state geology map and classed in preparation for groundwater mapping.

Drainage density

Drainage, which is plainly apparent on remote sensing imaging, is one of the most significant indicators of groundwater potential because the underlying lithology controls drainage pattern, texture, and density in a fundamental way (Falebita et al. 2020; Omosuyi et al. 2021). The drainage pattern reflects the pace at which precipitation infiltrates in comparison with surface runoff. High drainage density suggests an adverse location for groundwater existence, moderate drainage density indicates intermediate groundwater potential; and less or no drainage density indicates a good site for groundwater existence. The drainage pattern can be created using the SRTM DEM, and a drainage density map can be realized. The map generated can then be categorized to delineate groundwater. The drainage density η per kilometer used in geospatially estimating the map in the study is given by Eq. (6):

$$\eta = \frac{L}{A}, \quad (6)$$

where L is the total length of channel in kilometer and A is the areal expanse of the study in square kilometer.

Lineaments

Lineaments and their intersections provided information on the occurrence, transport, and storage of groundwater and are hence useful guides for delineation of groundwater potential. Many groundwater exploration operations in many nations have recently had greater success rates when drilling locations were guided by lineament mapping (Arshad et al. 2020). Lineament density maps were created and classed using the spatial analyzer tool.

Weighting of thematic maps using the Analytic Hierarchy Process (AHP)

AHP is a basic mathematical matrix-based approach that allows for intuitive determination of the relative weight of numerous criteria (Mogaji et al. 2021). AHP streamlines the decision-making process by letting the decision-maker focus on one aspect of the choice at a time (Ifediegwu 2022; Ghosh et al. 2022). This simplicity streamlines the decision-making process and makes it more transparent. AHP therefore provides a method of organizing decisions (Table 2), priorities, and judgments by allowing the decision maker to arrange them in a hierarchy with the highest priority, or objective, at the top. It also includes systematic checks on judgment consistency, which is one of its main advantages over other multi-attribute value systems (Ejebu et al. 2017; Gohsh et al. 2022; Thapa et al. 2017). This consistency testing allows for the comprehension of inconsistent judgments. Because the method is

adaptable, the decision maker can modify their priorities to ensure consistency. A matrix with a consistency ratio (CR) that is greater than 0.1 is often required for re-evaluation. All discovered themes in this study were evaluated against each other in a pairwise comparison matrix, which is a metric to represent the relative preference amongst the parameters in terms of groundwater occurrence, transportation, and storage as given in Table 2.

Normalization of assigned weights utilizing AHP (Wind and Saaty 1980) on Saaty’s scale examined two themes and classes at a time based on their respective relevance to identify groundwater potentials and recharging zone. Following that, AHP was used to build pairwise comparison matrices with specified weights to various thematic layers and classes, and the weights were normalized using the eigenvector technique. The consistency ratio (CR) was calculated according to Wind and Saaty (1980) in order to evaluate the normalized weights of various thematic layers and their specific classes. The following steps were taken to compute the CR of various thematic layers and their classes:

Square matrix: $A = a_{ij}$ [Eq. (7)], the element of row i column j was produced and the lower triangular matrix L_{ij} was completed by taking the reciprocal values of entries of the upper diagonal using the expression $(L_{ij} = \frac{1}{a_{ij}})$.

$$A = \begin{bmatrix} p_1 & p_1 & p_1 \\ p_1 & p_j & p_m \\ p_i & 1 & p_i \\ p_n & p_n & p_n \\ p_1 & p_j & p_n \end{bmatrix} \tag{7}$$

To get normalized relative weight, we divide each element of matrix $a_{ij} = \frac{p_i}{p_j}$ by Eq. (7) to obtain Eq. (8):

$$\frac{\frac{p_i}{p_j}}{\frac{\sum_{i=1}^n p_i}{p_i}} = \frac{p_i}{p_j} \times \frac{p_j}{\sum_{i=1}^n p_i} = \frac{p_i}{\sum_{i=1}^n p_i} \tag{8}$$

Averaging across the rows to get the normalized principal eigenvector (priority vector), i.e., Rate (R_i) or weight of row i (W_i) Eq. (9) resulted. Since it is normalized, the sum of all elements in the priority vector should be one.

$$\frac{W_i}{R_i} = \left[\frac{P_i}{\sum_{i=1}^n P_i} \dots \dots + \dots \frac{P_i}{\sum_{i=1}^n P_i} \right] \times 1/n \tag{9}$$

To compute λ_{max} , first multiply the normalized value by the respective weight and then, the values of the product are added together to get:

$$\lambda_{max} = \frac{C_1 + C_2 + C_3 \dots C_n}{n} \tag{10}$$

where C_1 to C_n are the λ value and n is the number of criteria. In this research, a λ_{max} value of 5.1966 was obtained.

Consistency index is a measure of consistency or degree of consistency of the judgment and computed using:

$$C_i = \frac{(\lambda_{max} - n)}{n - 1} \tag{11}$$

where n is the number of criteria considered. A consistency index value of 0.04915 was obtained in this study. The judgments of the pairwise comparison within each thematic layer were checked by the consistency ratio (CR) (Wind and Saaty 1980). The value of CR was computed by Eq. (12):

$$CR = \frac{C_i}{RCI} \tag{12}$$

where C_i is the consistency index, RCI is the Saaty’s ratio index which is computed by Saaty (1987), and for 5 variable, RCI value is 1.12. Computed CR obtained in this study is 0.04388. If the value of the CR is equal or less than 0.10, the inconsistency is acceptable. On the other hand, judgments should be revised if the CR is equal or greater than 0.10. The final map was achieved by overlaying all thematic maps using weighted overlay methods after assigning rates for classes in a layer and weights for thematic layers (Tamiru and Wagari 2021; Girma 2022). The groundwater potential index (GWPI) was estimated using the spatial analysis tool in ArcGIS 10.8 through Eq. (13):

$$GWPI = \sum_{i=1}^n W_i \times R_i \tag{13}$$

where W_i is the weight for each thematic layer and R_i is the rates for the classes within a thematic layer derived from AHP.

Results and discussion

Vertical electrical sounding (VES) data and hydraulic parameters

The general statistics of the VES data results for the locations is presented in Table 1. The results provide information on the primary geo-electric indices (layer resistivities, thickness and depths). The input layers for 19 VES points have been used to assess the outcomes from hydro-geophysical parameters, which are shown in Table 3. The ground truthing constrained interpretation of VES data performed using manual and electronic procedures gave the VES curves with their geologic dependent characteristics given in Fig. 2. The constraint of interpretation with VES data ensured fidelity in the interpreted primary geo-electric indices (Uwa et al. 2019). The inferred results identified geological units with layers ranging from three to four layers. The results in

Table 1 showcased the resistivity with the average of 512.4 Ωm and range of 21.0 to 1532.6 Ωm in the first layer. The second and third layers have resistivity ranges and mean values as 63.3–3688.7 Ωm and 167.4–2984.5 Ωm and 935.2 and 1112.6 Ωm , respectively. The fourth layers have average resistivity of 543.0 Ωm and range of 61.6–1188.0 Ωm . In terms of thickness, layers 1–3 have ranges as 1.0–36.3 m, 8.0–247.7 m and 52.6–151.2 m, respectively, while their corresponding mean values are 7.2 m, 66.2 m and 93.2 m. The inverted depths of investigation for layers 1 to 3 have respective ranges of 1.0–36.3 m, 9.0–250.0 m and 63.9–165.4 m and their corresponding mean of 7.2 m, 37.8 m and 105.9 m. The values of thickness and depth of investigations were not defined in layer 4 at the maximum current electrode separations (Uwa et al. 2019; Thomas et al. 2020). The distributions of resistivities from top to bottom of depth of investigations indicate the presence of facies changes within the study area. From the available ground truth data, the topmost layer is motley in compositions and the subsurface is characterized by fine to gravely sands with negligible intercalations of argillites, a typical geologic composition of Benin Formation in the Niger Delta (Akpan et al. 2020a, b). The lithofacies changes delineated reflect clay ($\rho < 100 \Omega\text{m}$), sandy clay ($100 > \rho < 100 \Omega\text{m}$), fine sands, ($400 > \rho \leq 1000 \Omega\text{m}$),

medium grained sands ($1000 > \rho \leq 1500 \Omega\text{m}$) and gravelly sands ($1500 \rho < 4000 \Omega\text{m}$). These high and low lithofacies indicate the variability in geologic units and hydraulic flow units in the study area (Umoh et al. 2022). The aquifer thickness reflects the volume of groundwater in the subsurface. Areas with the same thickness could be described in terms of isopach. Figure 4a and Table 3 reveal five major groups (50–92 m, 92–134 m, 134–177 m, 177–219 m, 219–262 m) of aquifer thicknesses delineated. The hotspot of the aquifer thickness clustered around VES 8, VES 14 and VES 15, which have the highest aquifer thickness in the range of 219–262 m. Aquifer depth refers to the location of groundwater in the subsurface. Areas with the same depth could be described in terms of Isopach. Figure 4b and Table 3 reveal five major groups: 51.48–94.13 m, 94.13–136.78 m, 136.78–179.43 m, 179.43–222.09 m and 222.09–264.74 m of aquifer depth inferred. The hotspot of the aquifer depth clustered around VES 9, VES 14 and VES 15, which have the highest aquifer depth in the range of 222.09–264.74 m. As all rocks have resistivities comparable to their nature and contents, rock units that make up aquifer resistivities are relatively high. The resistivities depend on the curve shapes of the VES data and model, which is dependent on geology of the place. This invariably means that there is no specific

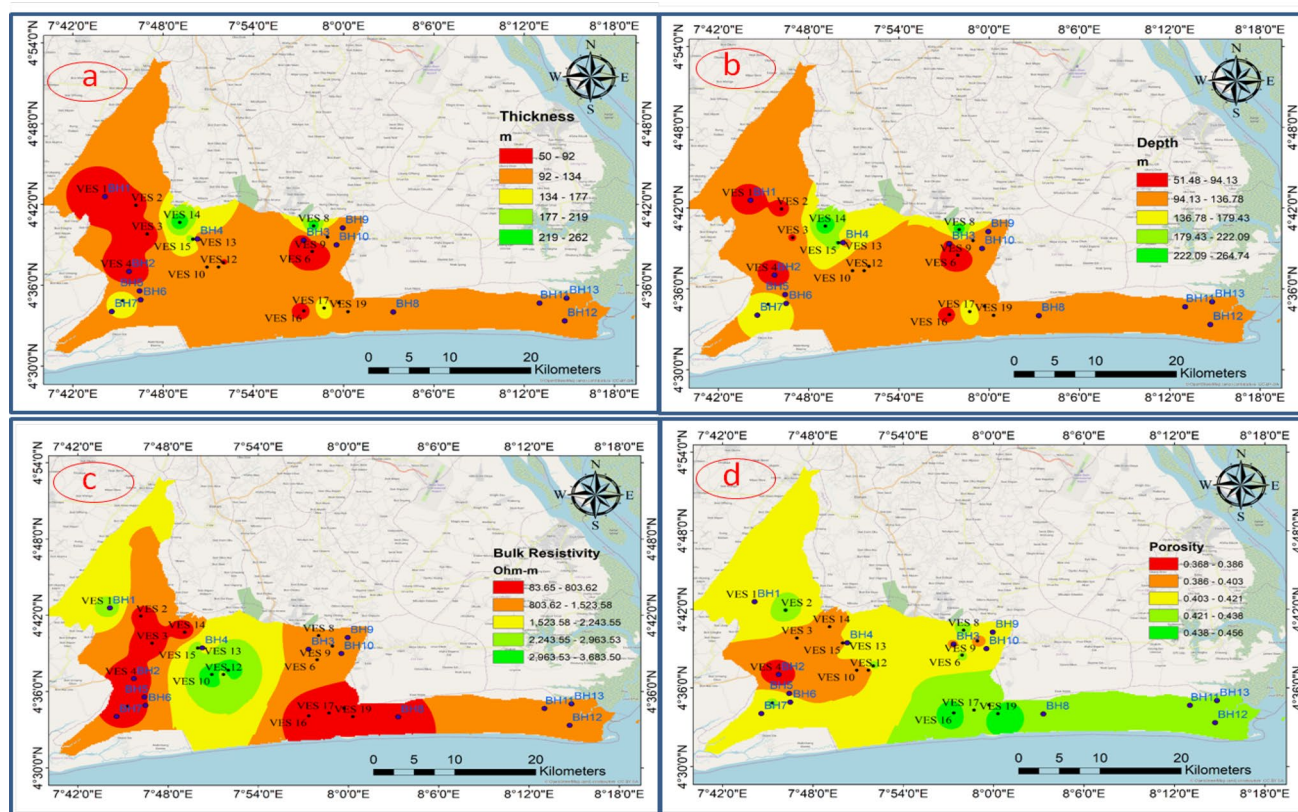


Fig. 4 Image map showing distribution **a** aquifer thickness, **b** aquifer depth, **c** aquifer resistivity, and **d** aquifer porosity distribution in the study area

range of aquifer resistivities (George 2021a). The aquifer resistivities vary between $83.65 \Omega\text{m}$ and as high as $3683.50 \Omega\text{m}$ (Table 3 and Fig. 4c). It can be observed that the highest aquifer resistivities in this area range from 2963.53 to $3683.50 \Omega\text{m}$ and the areas with this range include: VES 10 and VES 12. The ratio of empty space to total volume, which is commonly represented as fraction or in percentage, is the aquifer's porosity (Fig. 4d and Table 3). Effective porosity, which measures the amount of linked void space to the total volume, is the space accessible for fluid to flow. How much water can be held in geological materials is determined by their porosity. Due to their porosity, groundwater is present in almost all rocks. VES 16 and VES 19 have the highest effective porosity and by implication permeability in the study area (Ekanem et al. 2022b).

Based on the estimation of economic parametric properties, it is observed that hydraulic conductivity of the area

is highest around the southeastern part of the study area where the greatest hydraulic conductivity is about 3.43 m/day around VES 1, 4, 16, 17 and 19 (Fig. 5a and Table 3). The hydraulic conductivity K_h values in the southeastern part of the study area are high, and this indicates aquifers of good potentials (Ekanem et al. 2022a). As hydraulic conductivity is a measure of the ease at which groundwater flows, it is directly related to the lithology of the location and again the resistivity and transmissivity of the place. High hydraulic conductivity is also a function of the depth or aquifer thickness. The values in Fig. 4a were derived from the locations where hydraulic heads of some places were measured and others were statistically extrapolated. It can be deduced for nearby locations or places of uniform geology where any measurement has not been done.

The transmissivity of the study area is shown in the map of Fig. 5b and Table 3. The values are in the range of $71\text{--}687$

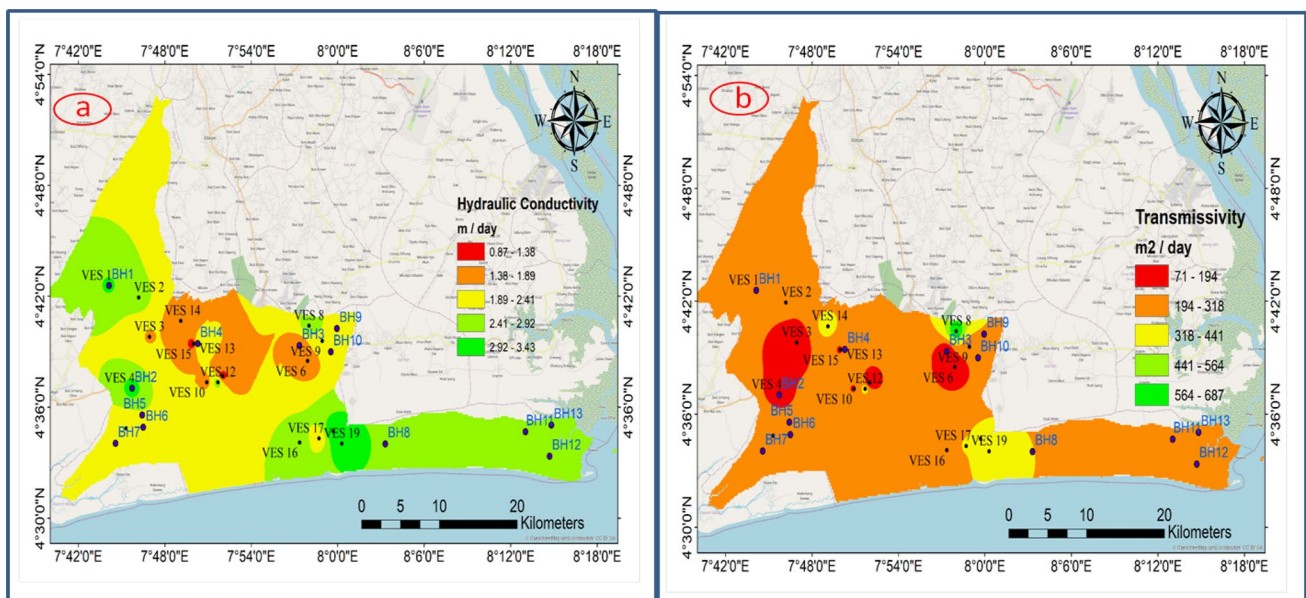
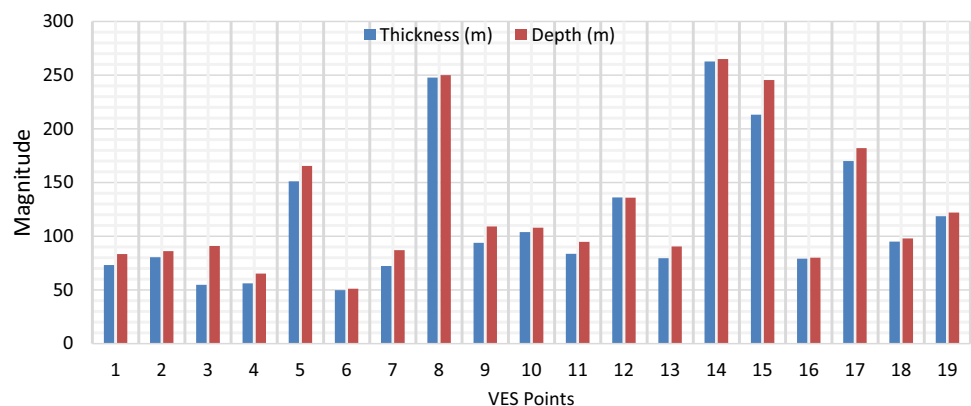


Fig. 5 Image map showing distribution **a** hydraulic conductivity and **b** transmissivity distribution in the study area

Fig. 6 Relationship between thickness and depth in the study area. There is little or no variation between the thickness and depth of the aquifers in the study area except in VES 3 and 15 as shown in Fig. 8. It is also observed that deeper aquifers have larger thickness within the study area



m^2/day . The transmissivity increases northward of the study area, with the eastern part having the lowest values of transmissivity. The highest values of transmissivity are found in VES 9, VES 14 and VES 19.

The chart in Fig. 6 shows that there is little or no variation between the thickness and depth of the aquifers in the study area except in VES 3 and 15. It is also observed that deeper aquifers have larger thickness within the study area. This finding is in line with Ibuot et al. (2019) and George (2020).

Conversely, the aquifer bulk resistivity is highly variable within the study area with the highest value in VES 10. There exists no relationship between the transmissivity (the product of hydraulic conductivity and thickness) and bulk resistivity (Fig. 7) and hence the reason for the nonlinearity of transmissivity with resistivity in the study area. This shows that resistivity alone cannot be reliably used for groundwater potential prediction as obsessed by some drillers. Conductivity and thickness are very important in groundwater potential estimation. The findings of

this study also identified the relationship between porosity (fractional) and hydraulic conductivity (m/day) in the study area. According to the chart in Fig. 8, there is a fairly invariant porosity distributions indicating that the study area is made up of a suite of sands with minimally varying pore spaces within them. However, hydraulic conductivity, which also depends on porosity, is controlled by dynamic viscosity and mean grain size (Soupios et al. 2007). In a nutshell, while fractional porosity is fairly constant due to similarity in lithology, hydraulic conductivity shows remarkable variations at different points due to varying dynamic viscosity and grain size. Practically, this shows the distribution of porosity and its hydraulic conductivity at different locations. This can be used to show the degree of permeability of the aquifer repositories (Umoh et al. 2022). As observed, high values of porosity correspond to high hydraulic conductivity. This finding agrees with George et al. (2018) and Uwa et al. (2019). Specifically, VES 18 and 19 have the highest hydraulic conductivity

Fig. 7 Relationship between bulk resistivity and transmissivity in the study area

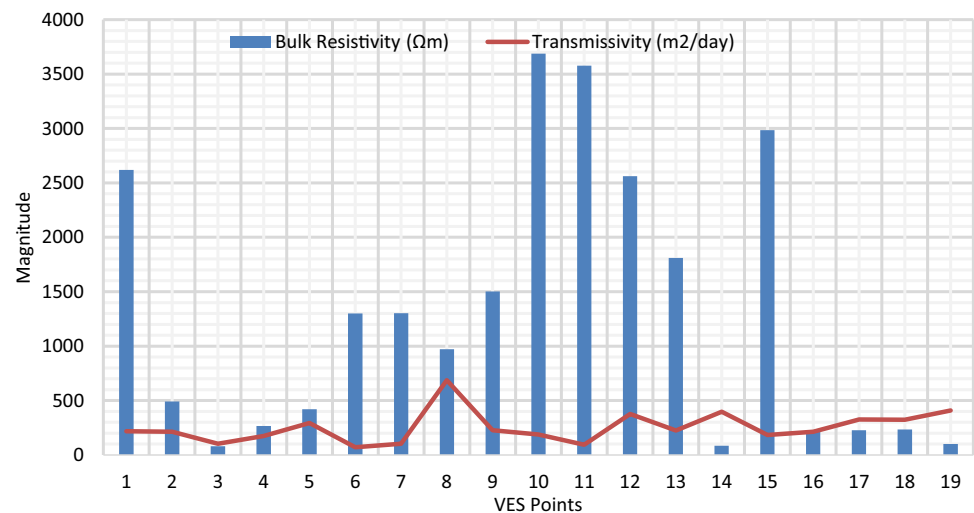


Fig. 8 Relationship between porosity (fractional) and hydraulic conductivity in the study area

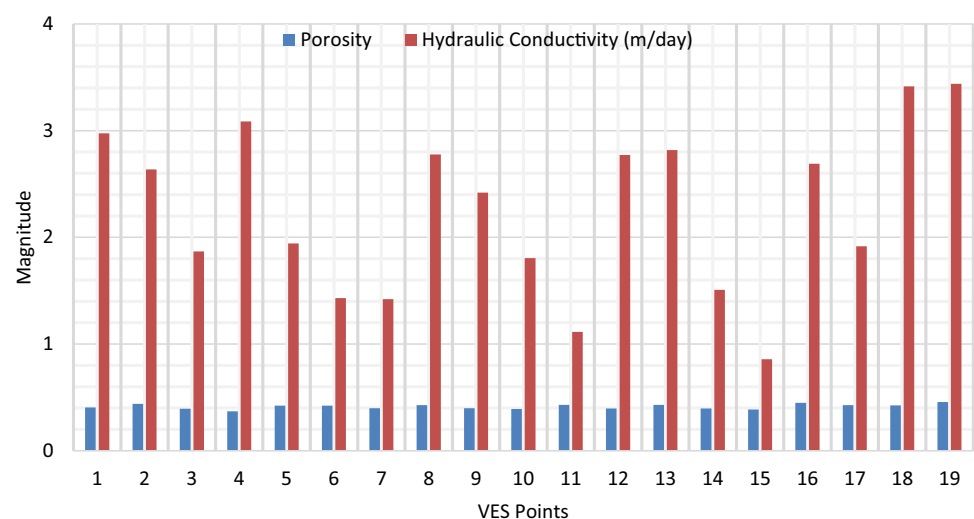


Table 4 Inferred classification and groundwater supply potential in the study area (Okogbue and Omonona 2013; Agbasi and Etuk 2016)

VES NO	Groundwater supply potential	Classification
1, 2, 3, 4, 5, 7, 8, 9, 10, 12, 13, 14, 15, 16, 17, 18 and 19	Withdrawal of lesser regional importance	High
6 and 11	Withdrawal of local water supply (small community, etc.)	Intermediate

value even though porosity remains fairly constant. This further shows that porosity is fairly sensitive to the pore system, while hydraulic conductivity, a quantitative measure of the capability of a geologic formation or other porous media to transport a specific fluid, is highly sensitive to the pore system (Soupios et al. 2007).

Based on the VES data analysis, Table 4 shows the groundwater potential and classification for the study area. From Table 4, VES stations 6 and 11 have intermediate and withdrawal of local water supply (small community, etc.) according to Okogbue and Omonona (2013) classification. All other VES points in the study area have high classification and withdrawal of lesser regional importance according to the classification.

RS and GIS analysis

Lineament and lineament density

Lineaments are linear features on the Earth's surface that indicate groundwater fissures on the surface. They are characterized as secondary porosity and may be detected on satellite photographs as tone shifts when compared to other topographical features (Suganthi et al. 2013; Sahu et al. 2022). A lineament can be a crack, fault, fracture, or master joint, as well as long and linear geological structures, topographic linearity, or the straight route of a stream. The previous studies have discovered a connection between lineaments and groundwater storage and flow (Mabee et al. 1994;

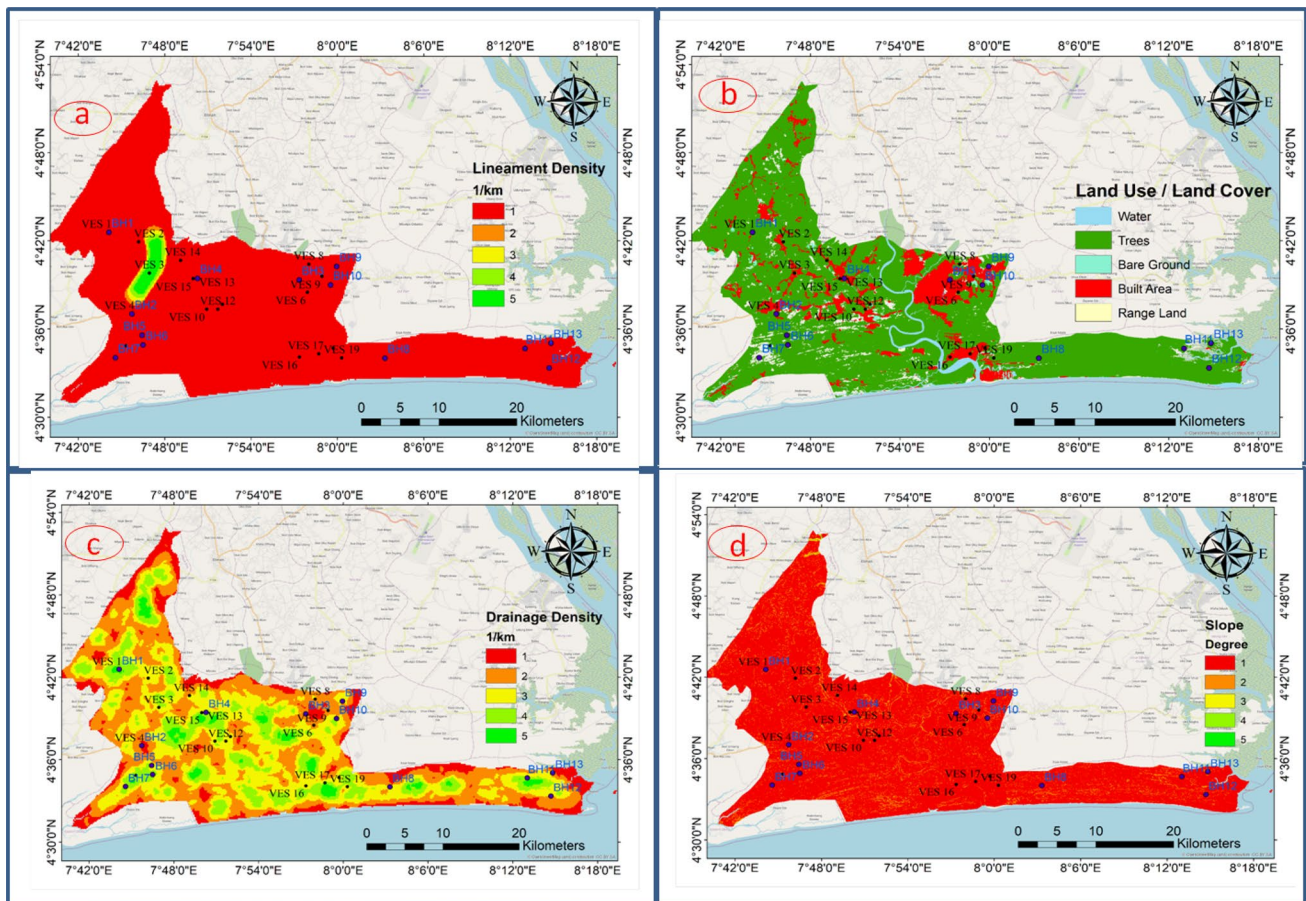


Fig. 9 Image map showing distribution of **a** reclassified lineament density, **b** land use/land cover, **c** drainage density and **d** slope in the study area

Magowe and Carr 1999; Solomon and Ghebreab 2006). The lineaments were imported into the ArcGIS environment, and the spatial analyst tool was used to build the lineament density map for the research region. Figure 9a depicts the lineament density map of the study area. A lineament density map is a quantitative length of linear feature per unit area that may indirectly reveal groundwater potential since the presence of lineaments typically indicates the existence of permeable units/layers. The line density tool was used to produce the lineament density from the lineament map of the research region. Higher lineament density polygons reflect more recharging and so have a better groundwater outlook (Solomon and Ghebreab 2006). The most important rating value was assigned to the largest lineament density period. Lineament junctions may also represent possible places of groundwater storage. As a result, places with high lineament density may have large groundwater possibilities. The map in Fig. 8a indicates uniformity in linear density (1 per kilometer) in all the VES points except VES 3, which has about 5 per kilometer.

Land use/land cover map

The occurrence of groundwater is influenced by the study area land cover and land use. Figure 9b illustrates the supervised classification of land use and land cover maps. According to the finding, three areas have the greatest area coverage in the research region. The built area is followed by water bodies and rangeland. Land usage and cover have an impact on runoff by either decreasing and assisting runoff or trapping water on plant leaves (Fan et al. 2022). Water droplets captured in this method fall to the ground and replenish groundwater. Land use/land cover may also have a detrimental impact on groundwater through evapotranspiration, assuming continual interception.

Drainage and drainage density maps

Figure 9c displays the research area drainage system. The drainage pattern was extracted straight from the DEM data. The type of vegetation, rainfall absorption capacity of soils, infiltration, and slope gradient have an impact on the drainage system, which is one of the most important indicators of hydrogeological features. The surface drainage density is defined as the ratio of total stream lengths to the grid area under consideration, and it is measured in per kilometer. A zone with a low drainage density promotes infiltration and decreases surface runoff (Cotton 1964; Lujijendijk 2022). Generally, low drainage density areas are suitable for groundwater development. The analysis in Fig. 8c indicates that study area has a range of 1–5 km^{-1} of drainage density with maximum areal spread occupied by low density between 1 and 2 km^{-1} and hence indicating significant groundwater potential (Ekanem et al. 2022a).

Slope maps

One of the factors controlling groundwater infiltration and recharge is slope. Thus, the kind of slope, in conjunction with other geomorphic parameters, may indicate the potential of groundwater in a certain place. Surface runoff is minor in low slope locations, allowing more time for rainwater infiltration, whereas heavy runoff occurs in high slope areas, limiting residence time for infiltration and recharging. In this study, the slope map (Fig. 8d) of the region was created using DEM data and the spatial analyst tool in ArcGIS. The slope map in Fig. 9d is generally 1° (one degree). This indicates the possibility for high infiltration and recharge, which leads to enhanced water potential in the area (Magesh et al. 2012).

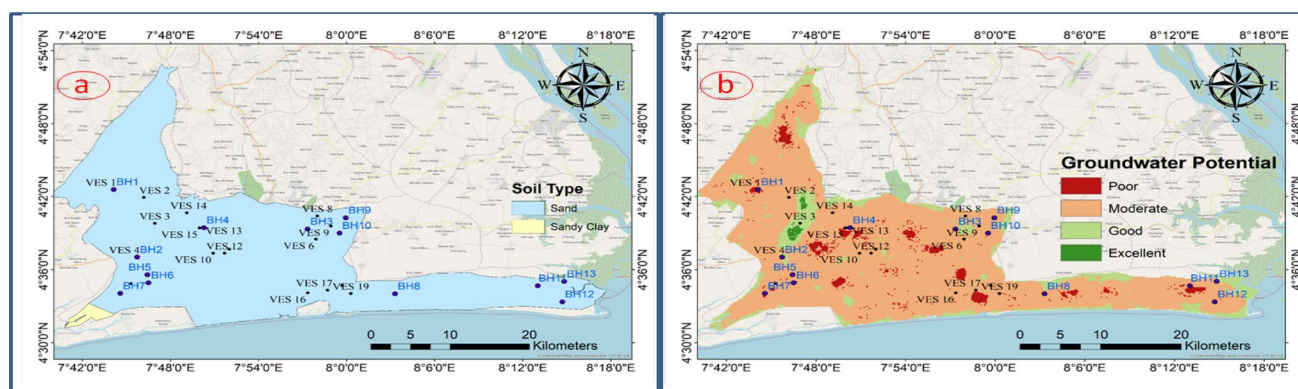


Fig. 10 Image map showing distribution of a soil type and b groundwater potential map of the study area

Soil type map

The soil type influences on both the porosity and permeability of aquifer rocks. The lithology layer was prepared by digitizing existing soil type map (Fig. 10a). The inferred soil type from RS is generally sandy with negligible sandy clay (Fig. 10a). This result from RS in Fig. 9a is also in line with the VES data results in Fig. 2. This suggests that the area is porous and permeable, and hence, it is characterized by high groundwater potential (Ekanem et al. 2022b).

Groundwater potential map

Integration of all thematic maps leads to the generation of groundwater potential index map in Fig. 10b. All the thematic maps of the elements influencing groundwater occurrence, transport, storage, and recharge were weighted and merged in an attempt to develop the basin's groundwater potential index (GPI) map. The image map in Fig. 10b depicts the RS generated map, and Table 5 shows the weights of the groundwater regulating elements. The image map shows four separate zones: poor, moderate, good and excellent. Furthermore, a thorough examination of the map indicates that the groundwater potential of the research region is mostly determined by lineament density, slope, and land use, in addition to soil type. The image also shows that places with significant groundwater potential are the northwestern parts of the area having high lineament density and between low and average slope. In general, the area has moderate to good groundwater potential index. This assertion from the work is in agreement with the work by Ikpe et al. (2022) and Ekanem et al. (2022a, b).

As inferred from analysis, the most important element, according to Table 5, was soil type (43%), followed by lineament density (33%), and slope (13%). Land use/land cover is the least major contributor to groundwater in the research region, accounting for about 4% of the total. The study CR determined to be 0.043884 is much lower than the 0.10 consistency threshold. In ArcGIS 10.8, the areal coverage of groundwater potential index was estimated by converting the potential to shapefiles and using the computation geometry

tool in the characteristics table to construct each potential zone.

The analytical hierarchy process (AHP) was used in a GIS setting to merge five thematic maps of elements influencing groundwater occurrence and movement using weighted overlay. The geometry calculator was used to estimate the groundwater potential coverage. Finally, the possible groundwater zones were evaluated using geophysical survey sites from several of the research survey area selected. According to the findings, soil type, lineament density, slope, drainage density, and land use/land cover have impacted on groundwater possibilities in the study region (Fan et al. 2022). The weightages of the parameters that determine groundwater prospects revealed that soil type was weighed the most (43%), followed by lineament density (33%), slope (13%), and drainage density (7%). With a weight of 4%, land use/land cover is the least significant contributor to groundwater in the research region. The CR for this study was calculated to be 0.04, which is much below the 0.10 consistency standard. The groundwater potential in the area surveyed is largely moderate, with a high potential within the study limits. Low and extremely low groundwater potentials are typically found in the southern reaches.

The groundwater potential index has been determined and classified into four categories: excellent, good, moderate, and poor potential. The study found that high groundwater potential index is concentrated in the northwestern part of the study area around VES 3 and in the boundaries of the study area. This study, which is in analogy with Sahu et al. (2022), has found significant regional diversity in groundwater potential within the study area. The variability observed is strongly related to the variability in the lithology, slope, drainage density, lineament density, and land use/cover (Mogaji et al. 2021). The most attractive prospective zone has low to average slope and a high lineament density. The work has shown generally low slope ($<2^\circ$) and variable lineament density ranging from 1 to 5 km^{-1} .

Validation of VES with RS and GIS

The validity of the result of RS and GIS technique was tested against the VES results. Cross-examination of the 19 VES

Table 5 Weights of groundwater factors used in the study

Parameters	Soil type	Lineament density	Slope	Drainage density	Land use/cover	Weight	Weight \times 100
Soil Type	1	2	3	6	8	0.43	43
Lineament Density	0.5	1	4	6	6	0.33	33
Slope	0.33	0.25	1	2	5	0.13	13
Drainage density	0.17	0.17	0.50	1	2	0.07	7
Land use/cover	0.13	0.17	0.20	0.50	1	0.04	4

Consistency ratio (CR) = 0.043884

Table 6 Groundwater potentiality from VES, RS and GIS in the study area

VES NO	Classification (VES)	Classification (RS and GIS)
1	High	Poor
2, 5, 8, 12, 13, 14, 15, 16, 17, 18, and 19	High	Moderate
3, 4, 7, 9, 10	High	Good
6	Intermediate	Moderate
11	Intermediate	Poor

geophysical surveyed points and the geospatial analyses was observed in the study. This was possible by overlaying the VES results on the groundwater potential map generated from the integration of various thematic maps estimated using multicriteria decision making. The attributes are summarized in Table 6 for the study area. The results showed maximally correlated and minimally infinitesimal uncorrelated relationships in the test groundwater potential parameters from VES data and the thematic geospatial data (RS and GIS). Out of the 19 points, only VES 1 and 11 points appeared to be grossly in disagreement in terms of groundwater potential among the electrical prospecting and spatiotemporal methods. This disagreement can be attributed to inherent departure of regional geology from local geology inferred from VES ground-based resistivity survey, vague multicriteria decision with deviation from normal or from the uniqueness in VES interpretation that is not screened by ground truth data (Adiat et al. 2012; Akpan et al. 2013). The result of overlay of the geophysical survey on the groundwater potential index obtained from the RS, GIS and VES technique in Table 5 showed reasonable seamless correlations in terms of groundwater potential with infinitesimal misfit expected to be due to obvious reason. The general results show that geospatially induced potential is in agreement with ground-based locally estimated potential and the hybridized map can be used seamlessly in groundwater exploration, exploitation or extraction.

Conclusion

The groundwater potential index has been derived in parts of Akwa Ibom State for the first time using contributions of electrical prospecting and spatiotemporal variations. The outcome showed that water repositories with high thickness and depths clustering around VES 9, VES 14, and VES 15 have the highest values ranging from 219 to 262 m and the highest aquifer depth in the range of 222.09–264.74 m. The highest aquifer resistivity in this area ranges from 2963 to 3683 Ω m. As inferred from analysis, the most important element was soil type (43%),

followed by lineament density (33%), and slope (13%). Land use/land cover is the least major contributor to groundwater in the research region, accounting for about 4% of the total. The study CR determined to be 0.043884 is much lower than the 0.10 consistency threshold and hence the justification of the results. The comparison of local information from surface geophysical technique (VES) and regional/spatiotemporal information from GIS-based multicriteria decision making (MCDM) and AHP methods to produce groundwater-potential maps of the study area using logical groups of characterizing hydrogeological entities has shown a striking uniformity in the hydrogeological study involving the potential of groundwater repositories in the study area. Aquifer systems have been classified into four categories, namely excellent, good, moderate and poor potential. It was observed from the study that high groundwater potential index is located in the southwestern part of the study area. However, the study showed that there is a relationship between the vertical electrical sounding (VES) and remote sensing results as the results of overlay and interplay between them showed that areas with high groundwater potential from VES analysis align with areas of good groundwater potential index map produced by GIS and RS. This study opined that there is a large spatial variability of groundwater potential within the study area. The variability inferred is closely followed by the variability in the soil type, slope, drainage density, lineament density and land use/cover of the study area. The most promising potential zone in the area is related to low slope and high lineament density which agreed perfectly with Fan et al. (2022). This study also showed in general that the groundwater potentiality increases with an increase in the thickness of the aquifer and depth for both GIS and remote sensing techniques and also with the electric resistivity method. This result, which agreed with George (2020) ground-based geophysical technique, can be used as reliable inputs in accessing sustainable groundwater mostly during dry seasons that durable water-bearing units seem to be issues to be considered in accessing groundwater within the economic depth of the study area.

Acknowledgements The authors are thankful to their colleagues in Geophysics Research Group (GRG) of Akwa Ibom State University for their assistance during the field data acquisition and editing of the manuscript.

Authors' Contributions NJG, OEA and AJU contributed to writing the original draft; resources; methodology; project administration; supervision. NJG, AME and JSE contributed to methodology, project administration; NJG, OEA, AJU, AME and JSE contributed to software, resources, data curation, and visualization. NJG, OEA, JET and IEU contributed to supervision, project administration, writing review, and editing; all authors read and approved the manuscript.

Funding The project was funded by the authors.

Declarations

Conflict of interest The authors declare that they have no known competing financial interests or personal relationships that could have appeared to influence the work reported in this paper.

Human and animal rights statement This article does not contain studies with human or animal subjects.

References

- Abdullateef L, Tijani MN, Nuru NA, John S, Mustapha A (2021) Assessment of groundwater recharge potential in a typical geological transition zone in Bauchi, NE-Nigeria using remote sensing/GIS and MCDA approaches. *Heliyon* 7:e06762
- Abdulrazzaq ZT, Agbasi OE, Aziz NA, Etuk SE (2020) Identification of potential groundwater locations using geophysical data and fuzzy gamma operator model in Imo, Southeastern Nigeria. *Appl Water Sci* 10(8):188
- Abdulrazzaq ZT, Agbasi OE, Alnaib AH, Asfahani J (2022) Determining the optimum drilling sites for groundwater wells based on the hydro-geo-electrical parameters and weighted overlay approach via GIS in Salah Al-Din Governorate, Central Iraq. *Iran J Geophys.* <https://doi.org/10.1155/2022/2682287>
- Adiat KAN, Nawawi MNM, Abdullah K (2012) Assessing the accuracy of GIS-based elementary multi criteria decision analysis as a spatial prediction tool—a case of predicting potential zones of sustainable groundwater resources. *J Hydrol* 440–441:75–89. <https://doi.org/10.1016/j.jhydrol.2012.03.028>
- Agbasi OE, Etuk SE (2016) Hydro-geo-electric study of aquifer potential in parts of Ikot Abasi Local Government Area, Akwa Ibom State, Using Electrical Resistivity Soundings. *Int J Geol Earth Sci* 2(4):43–54
- Agbasi OE, Aziz NA, Abdulrazzaq ZT, Etuk SE (2019) Integrated geophysical data and GIS technique to forecast the potential groundwater locations in part of South Eastern Nigeria. *Iraqi J Sci* 60(5):1013–1022
- Aizebeokhaia AP, Mohamed MM, Oladunjoye A, Mayowa BA, Bayo-Solarina OA, Sanuaded CE, Thompson FS, Ajayi O, Khaguere AE (2021) Evaluating the groundwater potential of coastal aquifer using geoelectrical resistivity survey and porosity estimation: a case in Ota SW Nigeria. *Groundw Sustain Dev* 12:100488
- Akpan AE, Ugbaja AN, George NJ (2013) Integrated geophysical, geochemical and hydrogeological investigation of shallow groundwater resources in parts of the Ikom- Mamfe Embayment and the adjoining areas in Cross River State, Nigeria. *Environ Earth Sci* 70(3):1435–1456. <https://doi.org/10.1007/s12665-013-2232-3>
- Akpan AS, Okeke FN, Obiora DN, George NJ (2020a) Modelling and mapping hydrocarbon saturated sand reservoir using Poisson's impedance (PI) inversion: a case study of Bonna field Niger, Delta Swamp Depobelt, Nigeria. *J Pet Explor Prod Technol* 11:117–132. <https://doi.org/10.1007/s13202-020-01027-8>
- Akpan AS, Obiora DN, Okeke FN, Ibuot JC, George NJ (2020b) Influence of wavelet phase rotation on post stack model based seismic inversion: A case study of X-field, Niger Delta, Nigeria. *J Pet Gas Eng* 11(1):57–67. <https://doi.org/10.5897/JPGGE2019.0320>
- Aladeboyeje AI, Coker J, Agbasi OE, Inyang NJ (2021) Integrated hydrogeophysical assessment of groundwater potential in the Ogun drainage basin, Nigeria. *Int J Energy Water Resour* 5(4):461–475
- Aretouyap Z, Asfahani J, Abdulrazzaq ZT, Tchato SC (2022) Contribution of the fuzzy algebraic model to the sustainable management of groundwater resources in the Adamawa watershed. *J Hydrol Reg Stud* 43:101198
- Arshad A, Zhang Z, Zhang W, Dilawar A (2020) Mapping favorable groundwater potential recharge zones using a GIS-based analytical hierarchical process and probability frequency ratio model: a case study from an agro-urban region of Pakistan. *Geosci Front* 11(5):1805–1819
- Arunbose S, Srinivas Y, Rajkumar S, Nair NC, Kaliraj S (2021) Remote sensing, GIS and AHP techniques-based investigation of groundwater potential zones in the Karumeniyar river basin Tamil Nadu, southern India. *Groundw Sustain Dev* 14:100586
- Biswajit D, Subodh CP (2020) Assessment of groundwater vulnerability to over-exploitation using MCDA, AHP, fuzzy logic and novel ensemble models: a case study of Goghat-I and II blocks of West Bengal India. *Environ Earth Sci* 79:104
- Cotton CA (1964) The control of drainage density. *NZ J Geol Geophys* 7(2):348–352. <https://doi.org/10.1080/00288306.1964.10420180>
- Ejegu JS (2020) Regional assessment of groundwater potential zone using remote sensing, GIS and multi criteria decision analysis techniques. *Niger Ann Pure Appl Sci* 3(3b):99–111
- Ejegu JS, Olasehinde P, Okhimamhe AA, Okunlola I (2017) Investigation of hydrogeological structures of Paiko region, north-Central Nigeria using integrated geophysical and remote sensing techniques. *Geosciences* 7(4):122
- Ejegu JS, Jimoh MO, Abdullahi S, Mba MA (2022) Groundwater exploration using multi criteria decision analysis and analytic hierarchy process in federal capital territory, Abuja, Central Nigeria. *Int J Geosci* 13(1):33–53
- Ejiogu BC, Opara AI, Nwosu EI, Nwofor OK, Onyema JC, Chinaka JC (2019) Estimates of aquifer geo-hydraulic and vulnerability characteristics of Imo State and environs, Southeastern Nigeria, using electrical conductivity data. *Environ Monit Assess* 191:238. <https://doi.org/10.1007/s10661-019-7335-1>
- Ekanem AM, George NJ, Thomas JE, Nathaniel EU (2020) Empirical relations between aquifer geohydraulic-geo-electric properties derived from surficial resistivity measurements in parts of Akwa Ibom State, Southern Nigeria. *Nat Resour Res* 29(4):2635–2646. <https://doi.org/10.1007/s11053-019-09606-1>
- Ekanem AM, Ikpe EO, George NJ, Thomas JE (2022a) Integrating geo-electrical and geological techniques in GIS-based DRASTIC model of groundwater vulnerability potential in the raffia city of Ikot Ekpena and its environs, southern Nigeria. *Int J Energy Water Resour.* <https://doi.org/10.1007/s42108-022-00202-3>
- Ekanem KR, George NJ, Ekanem AM (2022b) Parametric characterization, protectivity and potentiality of shallow hydrogeological units of a medium-sized housing estate Shelter Afrique, Akwa Ibom State, Southern Nigeria. *Acta Geophys.* <https://doi.org/10.1007/s11600-022-00737-3>
- Falebita D, Olajuyigbe O, Abeiya SS, Oche C, Ademola A (2020) Interpretation of geophysical and GIS-based remote sensing data for sustainable groundwater resource management in the basement of north-eastern Osun State Nigeria. *SN Appl Sci.* <https://doi.org/10.1007/s42452-020-03366-x>
- George NJ (2020) Appraisal of Hydraulic Flow Units and Factors of the Dynamics and Contamination of Hydrogeological Units in the Littoral Zones: A Case Study of Akwa Ibom State University and Its Environs, Mkpato Enin L.G.A., Nigeria. *Nat Resour Res* 29:3771–3788. <https://doi.org/10.1007/s11053-020-09673-9>
- George NJ (2021a) Geo-electrically and hydrogeologically derived vulnerability assessments of aquifer resources in the hinterland of parts of Akwa Ibom State Nigeria. *Solid Earth Sci.* <https://doi.org/10.1016/j.sesci.2021.04.002>
- George NJ (2021b) Integrating hydrogeological and second-order geoelectric indices in groundwater vulnerability mapping: A case study of alluvial environments. *Appl Water Sci* 11:123. <https://doi.org/10.1007/s13201-021-01437-x>

- George NJ, Ubom AI, Ibangi JI (2014) Integrated approach to investigate the effect of leachate on groundwater around the Ikot Ekpena Dumpsite in Akwa Ibom State, South-eastern Nigeria. *Int J Geophys*. <https://doi.org/10.1155/2014/174589>
- George NJ, Emah JB, Ekong UN (2015a) Geohydrodynamic properties of hydrogeological units in parts of Niger Delta, southern Nigeria. *J Afr Earth Sci* 105:55–63. <https://doi.org/10.1016/j.jafrearsci.2015.02.009>
- George NJ, Ibangi JI, Ubom AI (2015b) Geoelectrohydrogeological indices of evidence of ingress of saline water into freshwater in parts of coastal aquifers of Ikot Abasi, southern Nigeria. *J Afr Earth Sci* 109:37–46. <https://doi.org/10.1016/j.jafrearsci.2015.05.001>
- George NJ, Ibutot JC, Ekanem AM, George AMG (2018) Estimating the indices of inter-transmissibility magnitude of active surficial hydrogeologic units in Itu Akwa Ibom State, Southern. *Arab J Geosci* 11(6):1–16. <https://doi.org/10.1007/s12517-018-3475-9>
- George NJ, Umoh JA, Ekaname AM, Agbasi OE, Asfahani J, Thomas JE (2022) Geophysical-laboratory data integration for estimation of groundwater volumetric reserve of a coastal hinterland through optimized interpolation of interconnected geo-pore architecture. *J Coast Conserv*. <https://doi.org/10.1007/s11852-022-00902-2>
- Ghosh A, Adhikary PP, Bera B, Bhunia GS, Shit PK (2022) Assessment of groundwater potential zone using MCDA and AHP techniques: Case study from a tropical river basin of India. *Appl Water Sci* 12:37
- Girma D (2022) Identification of groundwater potential zones using AHP, GIS and RS integration: a case study of didessa sub-basin Western Ethiopia. *Remote Sens Land* 6:1–15. <https://doi.org/10.21523/gcjl.2022060101>
- Helena B, Pardo R, Vega M, Barrado E, Fernandez JM, Fernandez L (2000) Temporal evolution of groundwater composition in an alluvial aquifer (Pisuerga River, Spain) by principal component analysis. *Water Res* 34:807–816
- Ibangi JI, George NJ (2016) Estimating geohydraulic parameters, protective strength, and corrosivity of hydrogeological units: a case study of ALSCON, Ikot Abasi, southern Nigeria. *Arab J Geosci* 9:363. <https://doi.org/10.1007/s12517-016-2390-1>
- Ibutot JC, Akpabio GT, George NJ (2013) A survey of the repository of groundwater potential and distribution using geo-electrical resistivity method in Itu local government area (L.G.A.), Akwa Ibom State, southern Nigeria. *Central Eur J Geosci* 5(4):538–547. <https://doi.org/10.2478/s13533-012-0152-5>
- Ibutot JC, George NJ, Okwesili AN, Obiora DN (2019) Investigation of litho-textural characteristics of aquifer in Nkanu West Local Government Area of Enugu state, southeastern Nigeria. *J Afr Earth Sci* 153:197–207. <https://doi.org/10.1016/j.jafrearsci.2019.03.004>
- Ibutot JC, Aka MU, Inyang NJ, Agbasi OE (2022) Georesistivity and physicochemical evaluation of hydrogeologic units in parts of Akwa Ibom State, Nigeria. *Int J Energ Water Res*. <https://doi.org/10.1007/s42108-022-00191-3>
- Ifediegwu SI (2022) Assessment of groundwater potential zones using GIS and AHP techniques: a case study of the Lafia district, Nasarawa State, Nigeria. *Appl Water Sci* 12:10
- Ige AA, Coker J, Agbasi OE, Inyang N (2020) Hydrogeological appraisal of basement and sedimentary terrain in Ogun state using Geo-electrical methods. *Int J Adv Geosci* 8(1):95–101
- Ikpe EO, Ekanem AM, George NJ (2022) Modelling and assessing the protectivity of hydrogeological units using primary and secondary geo-electric indices: a case study of Ikot Ekpena Urban and its environs, southern Nigeria. *Model Earth Syst Environ*. <https://doi.org/10.1007/s40808-022-01366-x>
- Inim JJ, Udosen NI, Moshood NT, Afiah UE, George NJ (2020) Time-lapse electrical resistivity investigation of seawater intrusion in coastal aquifer of Ibeno, Southeastern Nigeria. *Appl Water Sci*
- Lee S, Lee CW (2015) Application of decision-tree model to groundwater productivity-potential mapping. *Sustainability* 7:13416–13432
- Li F, Wu J, Xu F, Yang Y, Du Q (2022) Determination of the spatial correlation characteristics for selected groundwater pollutants using the geographically weighted regression model: A case study in Weinan, Northwest China. *Hum Ecol Risk Assess Int J* 1–23
- Luijendijk C (2022) Transmissivity and groundwater flow exert a strong influence on drainage density Earth Surface. *Dynamics* 10(1):1–22. <https://doi.org/10.5194/esurf-10-1-2022>
- Mabee SB, Hardcastle KC, Wise DU (1994) A method of collecting and analyzing lineaments for regional-scale fractured-bedrock aquifer studies. *Ground Water* 32(6):884–894
- Machiwal D, Jha MK, Mal BC (2011) Assessment of groundwater potential in a semi-arid region of India using remote sensing, GIS and MCDM techniques. *Water Resour Manag* 25:1359–1386
- Magesh NS, Chandrasekar N, Soundranayagam JP (2012) Delineation of groundwater potential zones in Theni district, Tamil Nadu, using remote sensing, GIS and MIF techniques. *Geosci Front* 3(2):2189–2196
- Magowe M, Carr JR (1999) Relationship between lineaments and ground water occurrence in western Botswana. *Ground Water* 37(2):282–286
- Makonyo M, Msabi MM (2021) Identification groundwater potential recharge zones using GIS-based Multicriteria decision analysis: a case study of Semi-arid midlands Manyara fractured aquifer, North-Eastern Tanzania. *J Remote Sens Appl Soc Environ*
- Massoud MA, Fayad R, Kamleh R, El-Fadel M (2010) Environmental management system (ISO 14001) certification in developing countries: challenges and implementation strategies. *Environ Sci Technol* 44:1884–1887
- Mogaji KA, Ezekiel GI, Abodunde OO (2021) Modeling of aquifer potentiality using GIS-based knowledge-driven technique: a case study of hard rock geological setting, southwestern Nigeria. *Sustain Water Resour Manag* 7:64. <https://doi.org/10.1007/s40899-021-00538-4>
- Obinawu VI, George NJ, Udofia KM (2011) Estimation of aquifer hydraulic conductivity and effective porosity distributions using laboratory measurements on core samples in the Niger Delta, Southern Nigeria. *Int Rev Phys* 5(1):19–24
- Obiora DN, Ibutot JC, George NJ (2015) Evaluation of aquifer potential, geo electric and hydraulic parameters in Ezza North, south-eastern Nigeria, using geo-electric sounding. *Int J Environ Sci Technol* 13(2):433–444. <https://doi.org/10.1007/s13762-015-0886-y>
- Obiora DN, Ibutot JC, George NJ, Solomo UO (2016) Delineation of groundwater saturation indicators and their distributions in the complex argillaceous geological units of Ezza North Local Government Area of Ebonyi State Nigeria. *J Curr Sci*. <https://doi.org/10.18520/cs/v110/i4/701-708>
- Okogbue C, Omonona O (2013) Groundwater potential of the Egbe-Mopa basement area, central Nigeria. *Hydrol Sci J*. <https://doi.org/10.1080/02626667.2013.775445>
- Oli IC, Ahairakwem CA, Opara AI, Ekwe AC, Osi-Okeke I, Urom OO, Udeh HM, Ezennubia VC (2021) Hydrogeophysical assessment and protective capacity of groundwater resources in parts of Ezza and Ikwo areas, southeastern Nigeria. *Int J Energ Water Res* 5:57–72. <https://doi.org/10.1007/s42108-020-00084-3>
- Omosuyi GO, Oshodi DR, Sanusi SO, Igbagbo IA (2021) Groundwater potential evaluation using geoelectrical and analytical hierarchy process modeling techniques in Akure-Owode, southwestern Nigeria. *Model Earth Syst Environ* 7:145–158
- Pourtaghi ZS, Pourghasemi HR (2014) GIS-based groundwater spring potential assessment and mapping in the Birjand Township, southern Khorasan Province. *Iran Hydrogeol J* 22:643–662
- Reijers TJA, Petters SW, Nwajide CS (1997) The Niger delta Basin. In: Selley RC (ed) *African basins-sedimentary basin of the world*, vol 3. Elsevier Science, Amsterdam, pp 151–172

- Saaty TL (1980) The analytic hierarchy process. McGrawHill, New York
- Saaty RW (1987) (1987) The analytic hierarchy process-what it is and how it is used. *Math Model* 9:161–176
- Sahu U, Wagh V, Mukate S, Kadam A, Patil S (2022) Applications of geospatial analysis and analytical hierarchy process to identify the groundwater recharge potential zones and suitable recharge structures in the Ajani-Jhiri watershed of north Maharashtra, India. *Groundw Sustain Dev* 17:100733
- Short KC, Stauble AJ (1967) Outline of the geology of Niger Delta. *Assoc Petrol Geol Bull* 54:761–779
- Solomon S, Ghebream W (2006) Lineament characterization and their tectonic significance using Landsat TM data and field studies in the central highlands of Eritrea. *J Afr Earth Sc* 46(371):378
- Soupios PM, Kouli M, Vallianatos F, Vafidis A, Stavroulakis G (2007) Estimation of aquifer hydraulic parameters from surficial geophysical methods: a case study of Keritis Basin in Chania (Crete – Greece). *J Hydrol* 338:122–131. <https://doi.org/10.1016/j.jhydrol.2007.02.028>
- Suganthi S, Elango L, Subramanian SK (2013) Groundwater potential zonation by remote sensing and GIS techniques and its relation to the groundwater level in the coastal part of the Arani and Koratalai river basin, Southern India. *Earth Sci Res J* 17:87–95
- Tamiru H, Wagari M (2021) Evaluation of data-driven model and GIS technique performance for identification of groundwater potential zones: A case of Fincha Catchment, Abay Basin Ethiopia. *J Hydrol Reg Stud* 37:100902. <https://doi.org/10.1016/j.ejrh.2021.100902>
- Tang H, Schrimpf M, Lotter W, Moerman C, Paredes A, Caro JO, Hardesty W, Cox D, Kreiman G (2017) Recurrent computations for visual pattern completion. *Biol Sci* 115(35):8835–8840. <https://doi.org/10.1073/pnas.1719397115>
- Thapa R, Gupta S, Guin S, Kaur H (2017) Assessment of groundwater potential zones using multi-influencing factor (MIF) and GIS: A case study from Birbhum district, West Bengal. *Appl Water Sci* 7:4117–4131
- Thomas JE, George NJ, Ekanem AM, Nsikak EE (2020) Electrostratigraphy and hydrogeochemistry of hyporheic zone and water-bearing caches in the littoral shorefront of Akwa Ibom State University, Southern Nigeria. *Environ Monit Assess* 192(8):1–19. <https://doi.org/10.1007/s10661-020-08436-6>
- Todd DK (1980) Groundwater hydrology, 2nd edn. Wiley, New York
- Umoh JA, George NJ, Ekanem AM, Emah JB (2022) Characterization of hydro-sand beds and their hydraulic flow units by integrating surface measurements and ground truth data in parts of the shorefront of Akwa Ibom State, Southern Nigeria. *Int J Energy Water Resour*
- Uwa UE, Akpabio GT, George NJ (2019) Geohydrodynamic parameters and their implications on the coastal conservation: A case study of Abak Local Government Area (LGA), Akwa Ibom State, Southern Nigeria. *Nat Resour Res* 28(2):349–367. <https://doi.org/10.1007/s11053-018-9391-6>
- Vander Velpen BPA, Sporry RJ (1993) Resist: a computer program to process resistivity sounding data on PC compatibles. *Comput Geosci* 19(5):691–703
- Wind Y, Saaty TL (1980) Marketing applications of the analytic hierarchy process. *Manage Sci* 26:641–658
- Yiqun T, Jie Z, Ping YJ, Yan NZ (2017) Groundwater engineering. Springer Science and Business Media LLC, Berlin
- Younger PL (2007) Groundwater in the environment: an introduction Blackwell: London, Groundwater in the environment: an introduction, p 390
- Springer Nature or its licensor (e.g. a society or other partner) holds exclusive rights to this article under a publishing agreement with the author(s) or other rightsholder(s); author self-archiving of the accepted manuscript version of this article is solely governed by the terms of such publishing agreement and applicable law.